Virtual Colon: Spatiotemporal modelling of metabolic interactions in a computational colonic environment

Georgios Marinos[1,2]*, Johannes Zimmermann[1,3,4,5]*, Jan Taubenheim[1], and Christoph Kaleta[1,$]

[1] Research Group Medical Systems Biology, University Hospital Schleswig-Holstein Campus Kiel, Kiel University, Kiel, Schleswig-Holstein, Germany

[2] CAU Innovation GmbH, Kiel University, Kiel, Schleswig-Holstein, Germany

[3] Antibiotic resistance group, Max Planck Institute for Evolutionary Biology, Ploen, Schleswig-Holstein, Germany

[4] Evolutionary Ecology and Genetics, Zoological Institute, Kiel University, Kiel, Schleswig-Holstein, Germany

[5] Junior Research Group Mechanisms of Microbial Metabolic Interactions, Friedrich Schiller University Jena, Jena, Thüringen, Germany

*Shared first authorship with an interchangeable order

[$]Senior and corresponding author: c.kaleta@iem.uni-kiel.de

Georgios Marinos ORCID 0000-0002-6443-7696

Johannes Zimmermann ORCID 0000-0002-5041-1954

Jan Taubenheim ORCID 0000-0001-7283-1768

Christoph Kaleta ORCID 0000-0001-8004-9514

1. Abstract

Host-microbial metabolic interactions have been recognised as an essential factor in host health and disease. Genome-scale metabolic modelling approaches have made important contributions to our understanding of the interactions in such communities. One particular such modelling approach is BacArena in which metabolic models grow, reproduce, and interact as independent agents in a spatiotemporal metabolic environment. Here, we present a modelling application of BacArena, a virtual colonic environment, which reveals spatiotemporal metabolic interactions in a computational colonic environment. This environment resembles the crypt space together with the mucus layers, the lumen and fluid dynamics. Our proof-of-principle experiments include mono-colonisation simulations of context-specific colonic cells and simulations of context-specific colonic cells with the SIHUMIx minimal model microbiome. Our simulations propose host-microbial and microbial-microbial interactions that can be verified based on the literature. Most importantly, the Virtual Colon offers visualisation of interactions through time and space, adding another dimension to the genome-scale metabolic modelling approaches. Lastly, like BacArena, it is freely available and can be easily adapted to model other spatially structured environments (http://www.github.com/maringos/VirtualColon).

2. Introduction

Host-microbial interactions are of crucial importance for host health and fitness[1]. A well-studied example of localised host-bacterial interactions is the mammalian large intestine, where the gut microbiome provides the host with nutrients that otherwise would not be available to the host, protects it from colonisation by pathogens and interacts with its immune and nervous system[2]. For instance, some colonic bacteria can ferment fibres and other components in the colonic lumen. Subsequently, they produce short-chain fatty acids (SCFAs), such as acetate, butyrate and propionate that have diverse beneficial properties for host health[3,4]. Acetate and propionate are carried and utilised metabolically outside the intestine[5], while butyrate is used locally for energy generation[6]. However, their effect on the host is not only metabolic, as there is evidence of an interaction between SCFA and the immune system[7].

However, the case of SCFA is far from exceptional[8]. Therefore, it would be very informative to systematically explore host-microbial interactions inside the colonic microenvironment. In the colon, bacteria reside and are separated from the colonic tissue by two layers of a host-produced mixture of glycoprotein and oligosaccharides, collectively called mucus, which is located in between the lumen and the colonic epithelium[9]. This environment is characterised by the limited presence of oxygen fostering the growth of anaerobic bacteria under physiological conditions[10,11]. The bacteria consume dietary compounds that are not absorbed in the small intestine along with host-derived compounds such as mucus and bile[12]. Therefore, it is not surprising that the architecture of the colonic micro-environment offers a palette of well-studied localised host-bacterial interactions, as well as unknown ones.

Attempts to model this physicochemical environment and its phenomena in the intestine exist and are informative. For instance, Cremer and colleagues developed a mathematical, quantitative model that combines the microbes, their production of SCFA and colonic water absorption[13]. However, a promising method to understand novel,

unexplored host-microbial interactions is the modelling of the metabolism of both host and bacterial cells. Recent progress in the field of Systems Biology has enabled the creation of models of metabolism for a variety of organisms. Specifically, starting from the genomic information of individual species[14,15], it is possible to infer the possible metabolic pathways of the respective organisms and to organise them in networks of interconnected metabolic reactions, known as genome-scale metabolic models[16]. As a further step, we can apply mathematical methods, such as linear programming, to simulate the input and output of these networks. A common mathematical approach is flux balance analysis (FBA), which optimises the input and output of the models so that an objective function such as cell growth is maximised[17].

Simple metabolic models, such as the *Escherichia coli* core model with less than a hundred reactions, can be used to understand how the central metabolism of an organism operates[18]. For more advanced research, one can utilise existing curated models (e.g., the extensive, human-associated bacterial models collection AGORA2[19]) or even create own models tailored to the respective research question by employing modelling software such as gapseq and CarveMe[15,20]. Most importantly, it is possible to extend the layers of knowledge by combining datasets from different omics and databases, also beyond the strict boundaries of genome-scale metabolic modelling (e.g, see Virtual Metabolic Human database[21], MetaNetX[22–25], KEGG[26–28]). Emanating from this basis, spatiotemporal approaches that focus on simulating not only the models but also their environment through time have been developed[29]. For instance, an advanced approach by Versluis and colleagues has simulated how the metabolism of specific gut bacteria could alter based on the changes of the environment cues[30].

In this study, we build on the metabolic modelling software BacArena[31] which is an agent-based framework for spatial and temporal simulations of metabolic models. Specifically, it allows the design of a chemically defined environment, where the cells acting as agents can have predefined properties (e.g., speed, chemotaxis, linear or exponential growth etc.). Specifically, the models move, reside, duplicate, and die in a 2D space, where they can use the compounds around them. This setup allows the use of kinetic information, which is, however, difficult to obtain for nutritionally complex environments like the colon. To avoid unreasonably high uptake rates, the immediate surroundings of a microbial cell are modelled with appropriate dimensions that allow uptake in physiologically reasonable scales. In addition, parsimonious FBA is used to calculate the consumption and production of compounds as well as the production of biomass as an objective function over a defined time step. It provides the metabolic profile of each and every model in the simulation operating under steady state at a given time, including the consumption and production of metabolites by each bacterium. The 2D space is then updated in terms of new concentrations of compounds and addition (duplication) or removal of models. These time steps can hence be modelled iteratively, giving a numerical solution to the dynamics of growth and metabolism of the modelled system[16,31]. We present a virtual colon-like 2D and context-specific application of BacArena that combines the host and bacterial sides into one single simulation framework. Our implementation spatially separates bacteria and host cells by representing multiple mucus layers. Furthermore, it enables a realistic simulation of host and microbial interactions, as it combines spatial-dependent diffusion phenomena that constrain substrate availability and mimic the lumen faecal stream powered by peristalsis activity. Lastly, BacArena can be found online (http://www.github.com/euba/BacArena) and

it is required for running and adapting Virtual Colon. It is freely available on GitHub so that it can be easily adapted by future users (http://www.github.com/maringos/VirtualColon).

3. Material and methods

General setup

We conducted computational colonisation experiments mimicking an experimental setting with germ-free mice originally described by Geva-Zatorsky and colleagues (henceforward the reference study)[32]. Therefore, each simulation comprised bacterial models together with host models in our colon-like in-silico setting. Furthermore, each setting simulates seven iterations of one hour. The first iteration was used for the diffusion of compounds into the environment, to ensure that the compounds were well dispersed and readily available for uptake by the models. Subsequently, the simulation continued, combining metabolic models and diffusion In total, each setting was replicated ten times. The growth of each organism was calculated based on parsimonious flux balance analysis[33]. The majority of colonisation experiments referred to the introduction of one species (henceforward mono-colonisation). There were also three cases of specific-pathogen-free mice (SPF). In that case, we employed the generic simplified human intestinal bacterial community of eight species, whose initial relative abundance in the simulation was calculated based on experimental data(see Table 1, SIHUMIx)[34].

Metabolic models

In the case of the mono-colonisation experiments, bacterial metabolic models matching the bacterial strains of the reference study were used (see Supplementary Table S1)[32]. If a genome of a strain was not available, we took the most similar genome from NCBI and literature (see Supplementary Table S1)[35]. The genomes were utilised to create the respective bacterial metabolic models by gapseq (version ce962ff)[15]. The medium for gap filling was the one available in the lumen and mucus layers of the Virtual Colon (see Supplementary Table S1). The SIHUMIx metabolic models were reconstructed using gapseq (version 0e7af55)[15] based on the published genomic information by Becker and colleagues[34]. The gap-filling medium was predicted by gapseq. Finally, the models were adapted to grow on the medium available in the lumen and mucus layers of the Virtual Colon. Since we were interested in exploring the host-microbial interaction by finding the compounds that are exclusively of bacterial origin and taken up from the host cells, we had to exclude the possibility that the host cells use the dietary input of the bacterial models in parallel. Since host absorption primarily occurs in the small intestine and lumen content is therefore mainly available for microbial metabolism, we introduced a new "d" compartment into the bacterial models to account for an exclusive nutritional uptake of compounds from the lumen.

The host metabolic models originate from an adapted version of the published Recon 2.2 model[36]. This generic model was expanded so that a new compartment of exchange reactions was available. This compartment contains exchange reactions ending with “u” and is a copy of the original compartment of exchange reactions labelled “e”. The reason for this addition was to represent the flow of compounds between the bacteria in the lumen and the colonic cells (compartment “e”) and between the colonic cells and the

161 blood compartment (compartment "u"), following the strategy of Sahoo and Thelie[37].
162 Moreover, we used iMAT to integrate mouse transcriptomic data from the reference
163 study[32,38] into the host models[39] to build context-specific models of the respective colonic
164 tissue. After translating gene expression activity into reaction expression, a reaction was
165 assumed to be lowly expressed if it was within the first quartile of all reaction expression
166 values. A reaction was assumed to be highly expressed if it was in the fourth quartile across
167 all reaction expression values Moreover, we required a pre-set list of forced reactions and
168 unconstrained nutrition-related exchange reactions. This information was used as input to
169 determine a context-specific model for each condition. All exchange reactions and the
170 demand reaction for ATP "DM atp c" were available in the final models. It should be noted
171 that although Recon 2.2 is a human model, it was highly curated and was much more tested
172 than any specific mouse model at the time of simulations, while it requires less
173 computational power than its newer versions. Furthermore, there is little difference in
174 metabolic capacity between mice and humans[40], prompting us to use recon2.2 in our
175 modelling. Detailed information on the utilised models and the procedures can be obtained
176 from Table 1 and the models are available online (see Supplementary Table S1 and folder
177 'Supplementary Data S1', https://figshare.com/s/9a132d014cb58cb81559). Both the host
178 and bacterial models retained their original parameters unless otherwise specified.
179

180 Representation of the colon

181 The computational space of the Virtual Colon was developed by extending
182 BacArena, which provides a two-dimensional grid area[31]. One bacterial or host cell was
183 located in one grid cell. The size of the Virtual Colonic lumen, the mucus layers, and the
184 structure of the colonic crypts were calculated based on anatomic measurements converted
185 to the dimensions of one grid cell. Specifically, thanks to a predefined crypt-like position of
186 the host cells in the environment, two half-crypts were represented together with their
187 common inter-cryptal space (see Fig. 1 and Table 1).

188 The Virtual Colon is composed of five spaces: lumen, outer mucus, inner mucus,
189 intermediate space, host space. The inner mucus' width was equal to one-third of the total
190 mucus one, while the outer mucus' width was equal to two-thirds[41]. The concentration of
191 outer mucus layer compounds was found to be four times greater than that of the outer
192 ones[42] and was used accordingly (see Supplementary Table S2 for more information on
193 design, calculation, and further references). The bacterial models were introduced into the
194 colonic lumen and both mucus layers. The bacteria of the inner mucus were unable to move
195 unless the inner mucus was partially degraded. Then the bacterial models could move
196 through the grid cell and potentially pass towards the host. The bacterial models could not
197 enter human space, but they could be located next to the human models in the intermediate
198 space.

199 We started the simulations with reported abundances from the reference study [32].
200 The initial position of microbial cells in the Virtual Colon was random. Important additional
201 parameters were: the arena's size and volume, the actual total volume of the murine host's
202 caecum, colon and rectum (0.37 cm^3)[43], the bacterial input (200µl of 10^8 cfu/ml; personal
203 communication with Kasper Dennis ((dennis_kasper@hms.harvard.edu), corresponding
204 author of the reference study[32]). For instance, the amount of bacteria in the lumen was
205 calculated based on these formulas:

$$Amount_{lumen} = \frac{Area_{lumen} * Volume_{arena} * 0.2 * 10^{8}}{Area_{total}}$$

$$Volume_{arena} = Length_{Xaxis} * Length_{Yaxis} * \sqrt{Length_{Xaxis} * Length_{Yaxis}}$$

Similarly, the amount of bacteria in the outer and inner mucus areas was calculated. In the case of the SIHUMIx community simulations, the same approach was followed. However, an abundance factor accounting for the relative abundances of each species was used (see Table 1)[34].

The virtual host cells inherited the default human class settings of BacArena[31]. For the minimum weight and its standard deviation, the scaling factor was used to relate the area of human and bacterial cells. Rodriguez and colleagues have suggested that one crypt column is as long as 31.1 cells in the descending mouse colon[44]. Similarly, the two-crypt setting provided 70 model slots for host cells in total. Since the maximum allowed weight of 70 cells represented a maximum total weight of around all cells of a human crypt (BNID 110648[45]). In addition to these adjustments, no movement was allowed for the host models, and their growth was considered to be linear through time (see Table 1). As noted previously, the host models have the demand reaction for ATP "DM atp c"; therefore, it would have been possible to optimise the ATP maintenance instead of biomass. However, It should be noted that while there is some debate about whether optimisation of growth is an adequate objective function for flux balance simulations of colonic cells. The biomass function includes all molecular components of cells,also required for cell renewal. Furthermore, there is constant growth and shedding of colonic cells with an estimated turnover time of 3-5 days in mice[46]. Thus, in the colonic context, optimisation of growth is a valid objective function to predict metabolic fluxes.

The transport of molecules inside BacArena[31] was modelled by diffusion (see Supplementary Table S2). As discussed above, the arena was split into the following diffusion sectors: lumen, outer mucus layer, inner mucus layer, intermediate layer in-between, and blood. The utilised diffusion coefficients were calculated using a power regression function (coefficients vs. molecular weight) for the colonic lumen and mucus layers. The molecular weight was used for nutritional compounds. For other compounds, the default value of glucose was assumed. The regression functions were generated using the intestinal diffusion data of Winne and colleagues[47]. The same strategy was followed for the restricted areas and the lumen[48]. Especially for mucus layers, the diffusion coefficients of molecules in outer mucus were equal to ⅔ of mucus diffusion coefficients, while for inner mucus, they were equal to ⅓ of mucus diffusion coefficients, based on the observation that ⅓ of the length of the mucus belongs to the inner layer [41]. Furthermore, the mucus compounds were not allowed to diffuse to represent the stability of the mucus in the colonic environment. Oxygen could only diffuse to host areas to ensure limited "oxygenation" of the Virtual Colon. Practically, the diffusion of compounds in the lumen was designed to be less restricted than in mucus layers, while not possible in the intermediate layer and in blood. At the same time, diffusion of blood molecules was possible in the intermediate layer and in the blood.

Nutrition

Following the nutrition that was chosen by the authors of the reference publication [32], the primary source of nutritional compounds was the LabDiet ® JL Rat and Mouse/Auto 6F 5K67. These compounds were matched to the dietary bacterial exchange reactions to exclude nutritional competition between host and bacterial cells. The intestinal absorption and the dimensions of the Virtual Colon were considered for calculating the exact nutritional input. It is worth noting at this point that BacArena and, therefore, Virtual Colon is a simulation software that assumes that the concentration of the compounds can be used as the lower bounds of the respective exchange reactions. In addition to the LabDiet, some components such as water, H^+, minerals, vitamins, and mucus compounds were added as part of the lumen compartment. To represent the inflow of nutrients from the blood circulation, a minimal collection of compounds was added into the blood compartment. Their concentration was based on the literature (e.g., (BNID 110365[45]) and various Human Metabolome Database entries (https://hmdb.ca/[49–52]). To infer these components, a shadow cost analysis based on the BacArena [31] function "plotShadowCost" was utilised (see supplementary folder 'Supplementary Data S2', https://figshare.com/s/9a132d014cb58cb81559). A list of compounds can be found in the Supplementary Table S2.

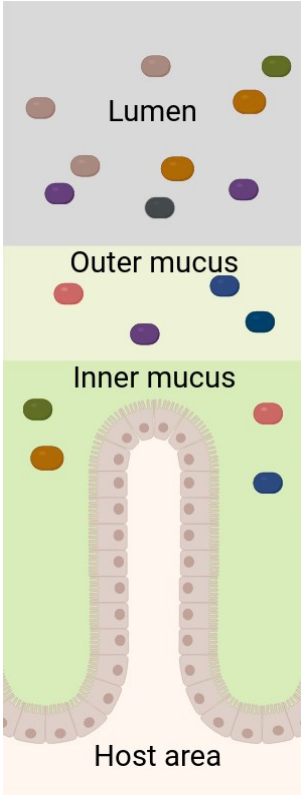

Figure 1: Schematic representation of the virtual colonic space. The coloured rectangles represent the models of the microbial species and the two shades of green represent the two mucus layers above the host's epithelium.Created in BioRender. Kaleta, C. (2025) https://BioRender.com/2pwtd0t.

Table 1: Overview of properties of the Virtual Colon

Property	Information on values & units	Further comments	Reference
Grid cell dimension	0.00025 × 0.00025 cm^2	Default in BacArena	31
Y-axis size	179-grid-cell-long	Set by the developers	Not applicable
X-axis size	24-grid cell-long	Set by the developers	NA
Scaling factor for minimum weight and its standard deviation of host models	132.73229:4.42	A human COLO205 colon cell has a diameter of 13 µm; hence its area is equal to 132.73229 μm^2. The area of a bacterium in BacArena is, by default, 4.42 μm^2.	45 BNID 108890
Scaling factor for maximum weight of host models	1000:70	70 cells represent the weight of around 1000 cells of a human crypt	44,45 BNID 110648[45]
Starting amount of bacteria in the lumen	29	Set by the developers	Not applicable
Starting amount of bacteria in the outer mucus	18	Set by the developers	Not applicable
Starting amount of bacteria in the inner mucus	9	Set by the developers	Not applicable
Initial relative abundance of *Anaerostipes caccae* in SIHUMIx simulations	0.1263867	Based on the concentration in human faeces [log10 cells / g dry matter]; see text	34
Initial relative abundance of *Bacteroides thetaiotaomicron* in SIHUMIx simulations	0.1444797	Based on the concentration in human faeces [log10 cells / g dry matter]; see text	34
Initial relative of *Bifidobacterium longum* in SIHUMIx simulations	0.1388008	Based on the concentration in human faeces [log10 cells / g dry matter]; see text	34
Initial relative of *Blautia producta* in SIHUMIx simulations	0.1385367	Based on the concentration in human faeces [log10 cells / g dry matter]; see text	34
Initial relative of *Clostridium butyricum* in SIHUMIx simulations	0.1065769	Based on the concentration in human faeces [log10 cells / g dry matter]; see text	34
Initial relative of *Clostridium ramosum* in SIHUMIx simulations	0.1263867	Based on the concentration in human faeces [log10 cells / g dry matter]; see text	34
Initial relative of *Escherichia coli* in SIHUMIx simulations	0.118859	Based on the concentration in human faeces [log10 cells / g dry matter]; see text	34
Initial relative of *Lactobacillus plantarum* in SIHUMIx simulations	0.09997359	Based on the concentration in human faeces [log10 cells / g dry matter]; see text	34

Software

The simulations and analyses thereafter presented in this manuscript were conducted in the R environment (version 4.2.1)[53]. Optimisations were generally conducted using the BacArena application (version 1.8.2, commit euba/BacArena@dc8e591 and euba/BacArena@008d186)[31] and sybil (version 2.2.1, commit SysBioChalmers/sybil@58eb989)[54]. The linear programming solver was CPLEX (academic version 22.1.0)[55], which is available through the R package cplexAPI (version 1.4.0)[56]. For data management, the software tidyverse (version 2.0.0) [57] and especially its library dplyr (version 1.1.4)[58] were used. For plotting, the software ggplot2 (version 3.5.1)[59], ggvenn (version 0.1.10)[60], ggthemes (version 5.1.0)[61], scales (version 1.3.0)[62], ggalluvial (version 0.12.5)[63], and BacArena (version 1.8.2, commit euba/BacArena@dc8e591)[31] were utilised. The software devtools (version 2.4.5) [64] was also used to manage the R environment.

The simulations were executed in the high-performance computing centre available at Kiel University as an array of independent tasks, each on a single CPU core. The longest running time was observed for the SIHUMI simulations, which included ten replicates running in a for-loop. A total runtime of 4.5 hours and a maximum memory usage of 6 GB were recorded. Although these data heavily depend on the randomly assigned node in the cluster, they are indicative of the performance and scalability of the setting. The underlying BacArena framework scales linearly with the number of individuals added (see also figure 2 in the BacArena manuscript [31]).

4. Results

The main objective of this study was to provide a computational framework to simulate host-microbial interactions in the mammalian colon. We first used our approach to study host-microbiome interactions in the colon based on a previously published dataset of single-strain colonisation experiments in germ-free mice[32]. Besides microbial abundance data, Geva-Zatorsky and colleagues provided extensive transcriptomic datasets of these colonisation experiments. Based on those transcriptomes, we reconstructed context-specific models of colonic tissue for the respective mice. For our study, we used context-specific Recon 2.2[36] host models along with bacterial models for joint simulations in a virtual colon.

The Virtual Colon provides detailed information on the host-microbial metabolic interactions in space and time. To reveal those interactions in the mono-colonisation experiments, we extracted all fluxes across all time points for each compound and for each model. Since a positive flux shows production and a negative one shows consumption of a compound, we calculated the sum of fluxes of all models for each compound. Collectively, the host models produced 20 compounds and the bacterial ones produced 27 compounds (Fig. 2A). Interestingly, the host-microbial interactions seem to be very pair-specific, since we could identify compounds that in some pairs are bacterially produced or in other pairs by the host (eg., glycine, L-alanine; Fig. 2A). Furthermore, we observed the host exchange of nitrogen-containing compounds, towards the bacterial models, and the uptake of bacterially produced SCFA. Additionally, we found that although the majority of the bacteria interacted metabolically with the host regardless of their position (e.g., see cases with fluxes of models originated from all three layers: lumen, outer mucus, inner mucus, Fig. 2B), we also observed cases of localised interactions (Fig. 2B).

Further, we employed the Virtual Colon to study host-bacterial interactions with the SIHUMIx bacterial community. As a proof-of-principle, we studied the growth patterns of the bacterial and host models. Each bacterial strain achieved different growth rates and all the models were still in the exponential phase at the end of simulation. The host cells did not reproduce, as expected (Fig. 3A). Regarding the different layers of Virtual Colon, there is a variation of growth rate of the bacterial models depending on their position in the colonic space (Fig. 3B). Inside the inner mucus layer they could only marginally spread in comparison to the other locations due to the design of the movement barrier. The SIHUMIx microbial community that resides in inner and outer colonic mucus also gradually consumed the mucus compound N-acetylneuraminate. Most interestingly, the decreasing quantity of the compound follows the growth of the bacteria models in the area. The bacterial models of *Bacteroides thetaiotaomicron*, *Blautia producta*, and *Clostridium butyricum* can degrade N-acetylneuraminate. (Fig. 3C).

The observation of microbial mucus degradation led to more general questions on what compounds are consumed or produced by the metabolic models. The host models, similarly to the mono-colonisation experiments, are context-specific Recon 2.2 models[36], whose reconstruction was based on the transcriptomes GSM2354402, GSM2354403 and GSM2354404 respectively. While those three models produce and consume mostly the same compounds, they do have distinct metabolic profiles that can be attributed to the different transcriptomes. For instance, the recon model GSM2354403 produced L-alanine, which was taken up by the bacteria, while the recon model GSM2354404 consumed bacterial L-alanine (Fig. 4A and 4D). However, all models consumed bacterially produced short-chain fatty acids, such as formate, acetate, propionate, and butyrate (Fig. 4C and 4D). Interestingly, the models exchange various metabolic compounds (e.g., water, vitamins, amino acids, TCA-cycle compounds such as alpha-oxoglutarate).

Not only were the bacterially produced compounds taken up by the host models, but they were also consumed by other bacterial species of the community (Fig. 5A and 5B). For instance, apart from amino acids and carbon sources, they also exchanged metabolites like protons, ammonium, phosphate, and hydrogen sulphide. It is possible to characterise the metabolic role of community members. The bacteria model of *E. coli* was the most active species in terms of production and consumption of compounds. On the other hand, *B. longum* and *C. butyricum* contributed more compounds than they consumed, while the opposite was true for *A. caccae* and *B. producta*.

Furthermore, in order to understand how the metabolic interactions change when comparing the interactions from mono-colonisation with the SIHUMIx simulations, we investigated which compounds are unique in each of the two settings. It can be observed that the exchanged compounds were mostly common (Fig. 6). However, the majority of the unique compounds in mono-colonisation experiments were nitrogen-containing compounds. In the other two parts of the Venn diagram, we could identify amino acids, metabolism intermediates (e.g. fumarate) and short-chain fatty acids.

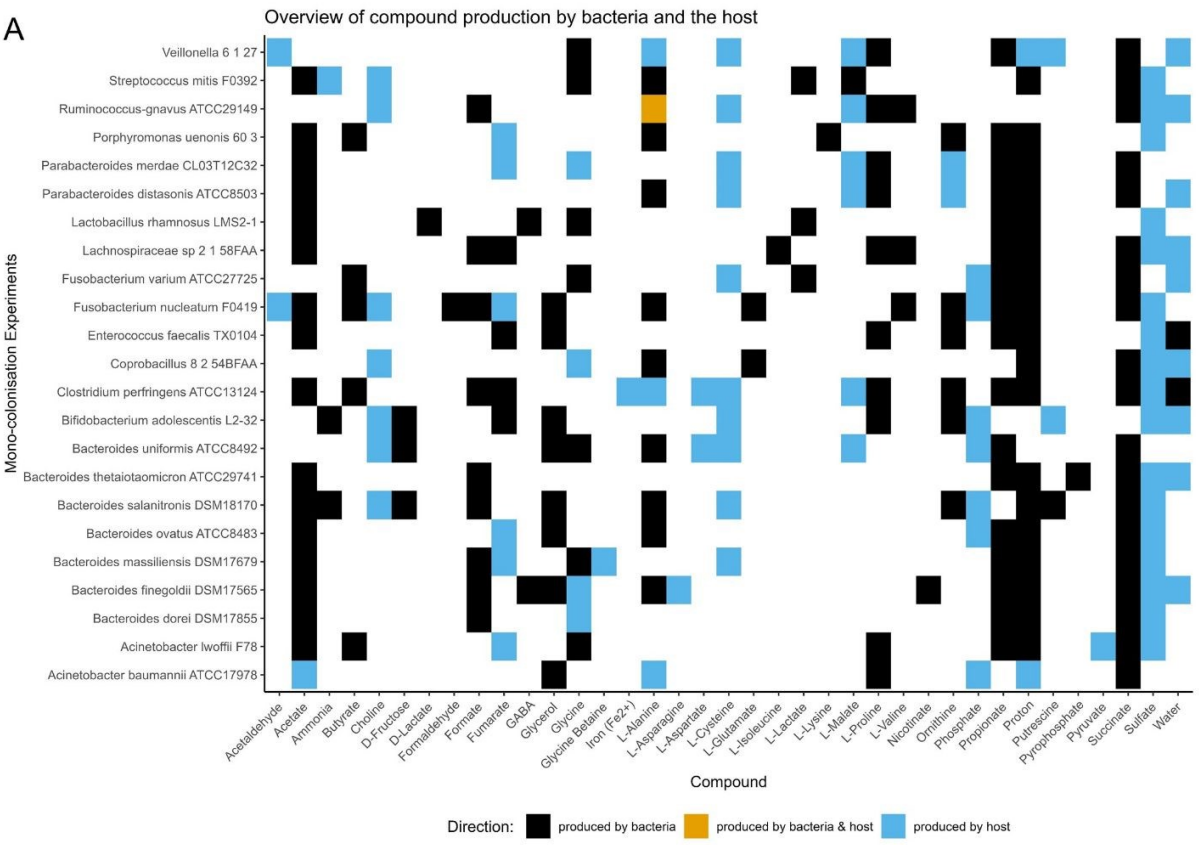
A
Overview of compound production by bacteria and the host
Mono-colonisation Experiments
Veillonella 6 1 27
Streptococcus mitis F0392
Ruminococcus-gnavus ATCC29149
Porphyromonas uenonis 60 3
Parabacteroides merdae CL03T12C32
Parabacteroides distasonis ATCC8503
Lactobacillus rhamnosus LMS2-1
Lachnospiraceae sp 2 1 58FAA
Fusobacterium varium ATCC27725
Fusobacterium nucleatum F0419
Enterococcus faecalis TX0104
Coprobacillus 8 2 54BFAA
Clostridium perfringens ATCC13124
Bifidobacterium adolescentis L2-32
Bacteroides uniformis ATCC8492
Bacteroides thetaiotaomicron ATCC29741
Bacteroides salanitronis DSM18170
Bacteroides ovatus ATCC8483
Bacteroides massiliensis DSM17679
Bacteroides finegoldii DSM17565
Bacteroides dorei DSM17855
Acinetobacter lwoffii F78
Acinetobacter baumannii ATCC17978
Acetaldehyde
Acetate
Ammonia
Butyrate
Choline
D-Fructose
D-Lactate
Formaldehyde
Formate
Fumarate
GABA
Glycerol
Glycine
Glycine Betaine
Iron (Fe2+)
L-Alanine
L-Asparagine
L-Aspartate
L-Cysteine
L-Glutamate
L-Isoleucine
L-Lactate
L-Lysine
L-Malate
L-Proline
L-Valine
Nicotinate
Ornithine
Phosphate
Propionate
Proton
Putrescine
Pyrophosphate
Pyruvate
Succinate
Sulfate
Water
Compound
Direction:
produced by bacteria
produced by bacteria & host
produced by host

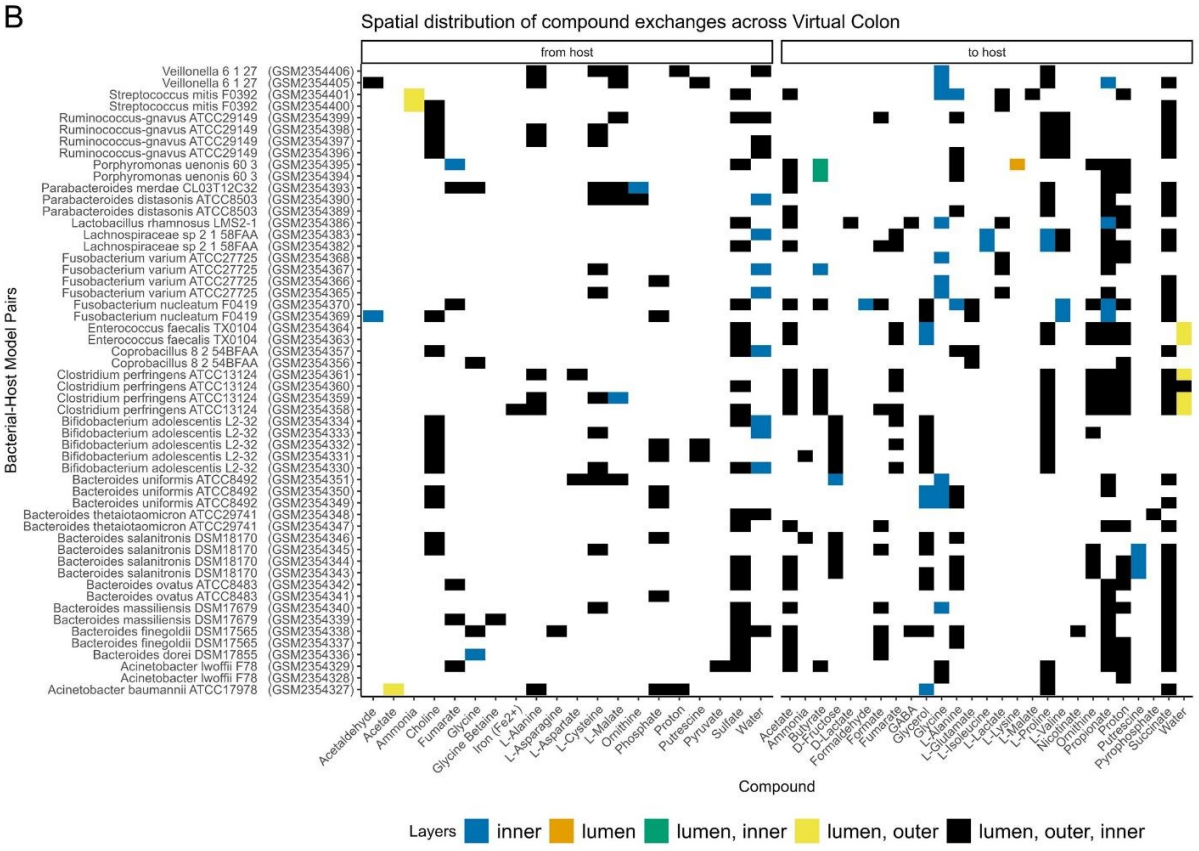
B
Spatial distribution of compound exchanges across Virtual Colon
from host
to host
Bacterial-Host Model Pairs
Veillonella 6 1 27 (GSM2354406)
Veillonella 6 1 27 (GSM2354405)
Streptococcus mitis F0392 (GSM2354401)
Streptococcus mitis F0392 (GSM2354400)
Ruminococcus-gnavus ATCC29149 (GSM2354399)
Ruminococcus-gnavus ATCC29149 (GSM2354398)
Ruminococcus-gnavus ATCC29149 (GSM2354397)
Ruminococcus-gnavus ATCC29149 (GSM2354396)
Porphyromonas uenonis 60 3 (GSM2354395)
Porphyromonas uenonis 60 3 (GSM2354394)
Parabacteroides merdae CL03T12C32 (GSM2354393)
Parabacteroides distasonis ATCC8503 (GSM2354390)
Parabacteroides distasonis ATCC8503 (GSM2354389)
Lactobacillus rhamnosus LMS2-1 (GSM2354386)
Lachnospiraceae sp 2 1 58FAA (GSM2354383)
Lachnospiraceae sp 2 1 58FAA (GSM2354382)
Fusobacterium varium ATCC27725 (GSM2354368)
Fusobacterium varium ATCC27725 (GSM2354367)
Fusobacterium varium ATCC27725 (GSM2354366)
Fusobacterium varium ATCC27725 (GSM2354365)
Fusobacterium nucleatum F0419 (GSM2354370)
Fusobacterium nucleatum F0419 (GSM2354369)
Enterococcus faecalis TX0104 (GSM2354364)
Enterococcus faecalis TX0104 (GSM2354363)
Coprobacillus 8 2 54BFAA (GSM2354357)
Coprobacillus 8 2 54BFAA (GSM2354356)
Clostridium perfringens ATCC13124 (GSM2354361)
Clostridium perfringens ATCC13124 (GSM2354360)
Clostridium perfringens ATCC13124 (GSM2354359)
Clostridium perfringens ATCC13124 (GSM2354358)
Bifidobacterium adolescentis L2-32 (GSM2354334)
Bifidobacterium adolescentis L2-32 (GSM2354333)
Bifidobacterium adolescentis L2-32 (GSM2354332)
Bifidobacterium adolescentis L2-32 (GSM2354331)
Bifidobacterium adolescentis L2-32 (GSM2354330)
Bacteroides uniformis ATCC8492 (GSM2354351)
Bacteroides uniformis ATCC8492 (GSM2354350)
Bacteroides uniformis ATCC8492 (GSM2354349)
Bacteroides thetaiotaomicron ATCC29741 (GSM2354348)
Bacteroides thetaiotaomicron ATCC29741 (GSM2354347)
Bacteroides salanitronis DSM18170 (GSM2354346)
Bacteroides salanitronis DSM18170 (GSM2354345)
Bacteroides salanitronis DSM18170 (GSM2354344)
Bacteroides salanitronis DSM18170 (GSM2354343)
Bacteroides ovatus ATCC8483 (GSM2354342)
Bacteroides ovatus ATCC8483 (GSM2354341)
Bacteroides massiliensis DSM17679 (GSM2354340)
Bacteroides massiliensis DSM17679 (GSM2354339)
Bacteroides finegoldii DSM17565 (GSM2354338)
Bacteroides finegoldii DSM17565 (GSM2354337)
Bacteroides dorei DSM17855 (GSM2354336)
Acinetobacter lwoffii F78 (GSM2354329)
Acinetobacter lwoffii F78 (GSM2354328)
Acinetobacter baumannii ATCC17978 (GSM2354327)
Acetaldehyde
Acetate
Ammonia
Choline
Fumarate
Glycine
Glycine Betaine
Iron (Fe2+)
L-Alanine
L-Asparagine
L-Aspartate
L-Cysteine
L-Malate
Ornithine
Phosphate
Proton
Putrescine
Pyruvate
Sulfate
Water
Acetate
Ammonia
Butyrate
D-Fructose
Formaldehyde
Formate
GABA
Glycerol
Glycine
L-Alanine
L-Glutamate
L-Isoleucine
L-Lactate
L-Lysine
L-Malate
L-Proline
L-Valine
Nicotinate
Ornithine
Propionate
Proton
Putrescine
Pyrophosphate
Succinate
Water
Compound
Layers
inner
lumen
lumen, inner
lumen, outer
lumen, outer, inner

Figure 2: A. Exchange of compounds which are produced by the bacterial models or context-specific host models. The colour of the layers depends on the origin of the producer. Multiple context-specific host models, each originating from a transcriptomic dataset of mono-colonisation experiments, were simulated per bacterial model. B. Spatial localisation of exchanges: exchange of compounds which are produced by the host models and are consumed by the bacterial model, and vice versa. Each row represents an independent set of simulations of a specific bacterial species with a distinct context-specific host metabolic model. The repetition of bacterial strain names (e.g., *Streptococcus mitis*) highlights that the same bacterial species was simulated with multiple context-specific host models, identified by their respective codes of the transcriptomic data (e.g., GSM235440 and GSM2354401). To estimate the exchange of compounds among the models, the sum of all fluxes across time for each compound and for each model was determined. A positive sum denotes production, while a negative one denotes consumption. To limit the numerical artefacts, the fluxes whose absolute value was less than 1E-6 were considered zero.

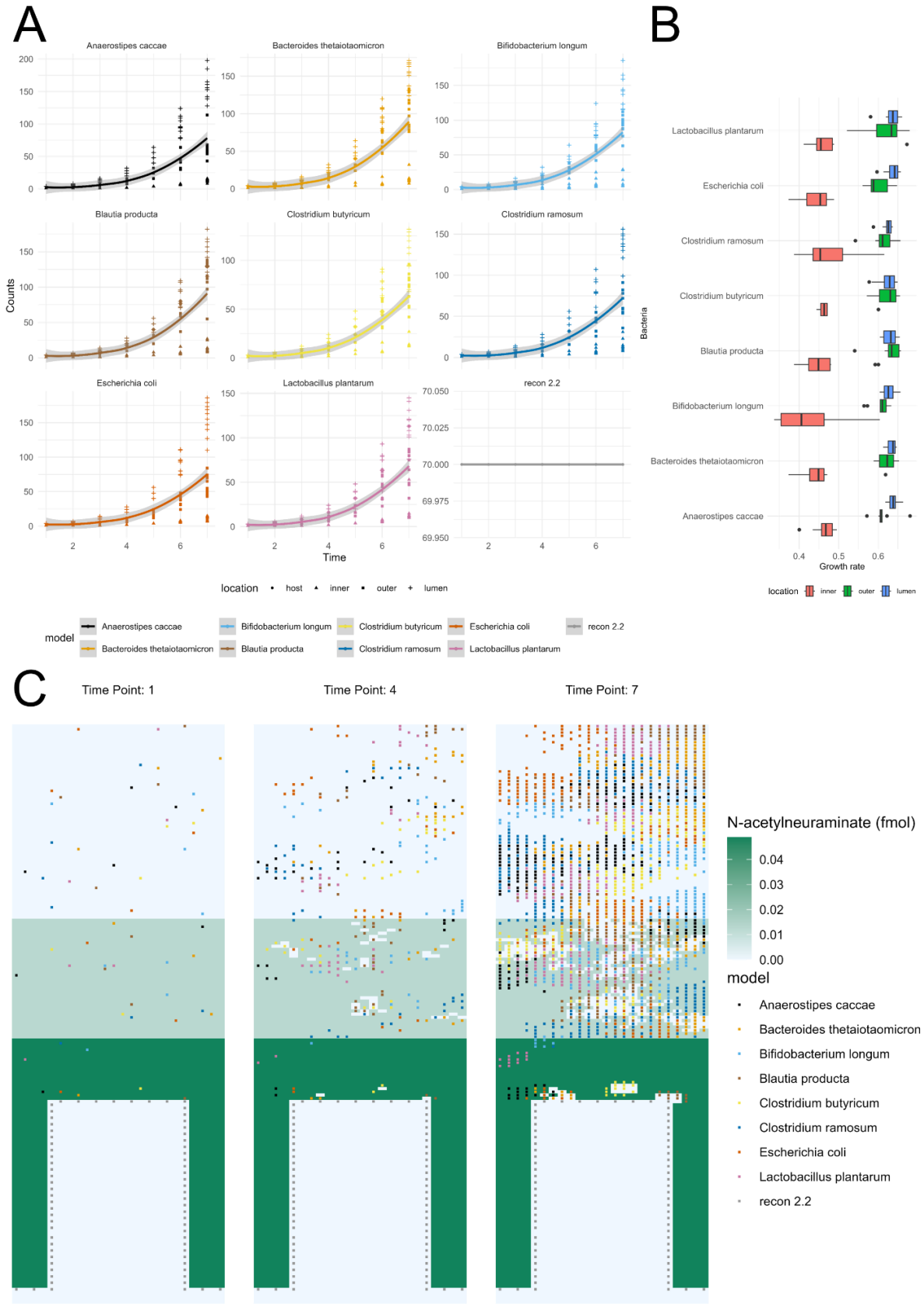

Figure 3: A. Growth curves for the individual bacterial and host models. The data points originate from all the replicates of the GSM2354402 SIHUMIx simulation. The individual lines

are plotted using the “loess” smoothing function. B. Variation in growth rates (unit h^{-1}) by location in Virtual Colon and Species. The growth rate Data points represent all replicates from the GSM2354402 SIHUMIx simulation. C. Schematic representation of the mucus compound N-acetylneuraminate through three-time points in a SIHUMIx-host simulation (GSM2354402, 10th replicate). Each subplot represents the substance concentration and bacterial population per time point in hours.

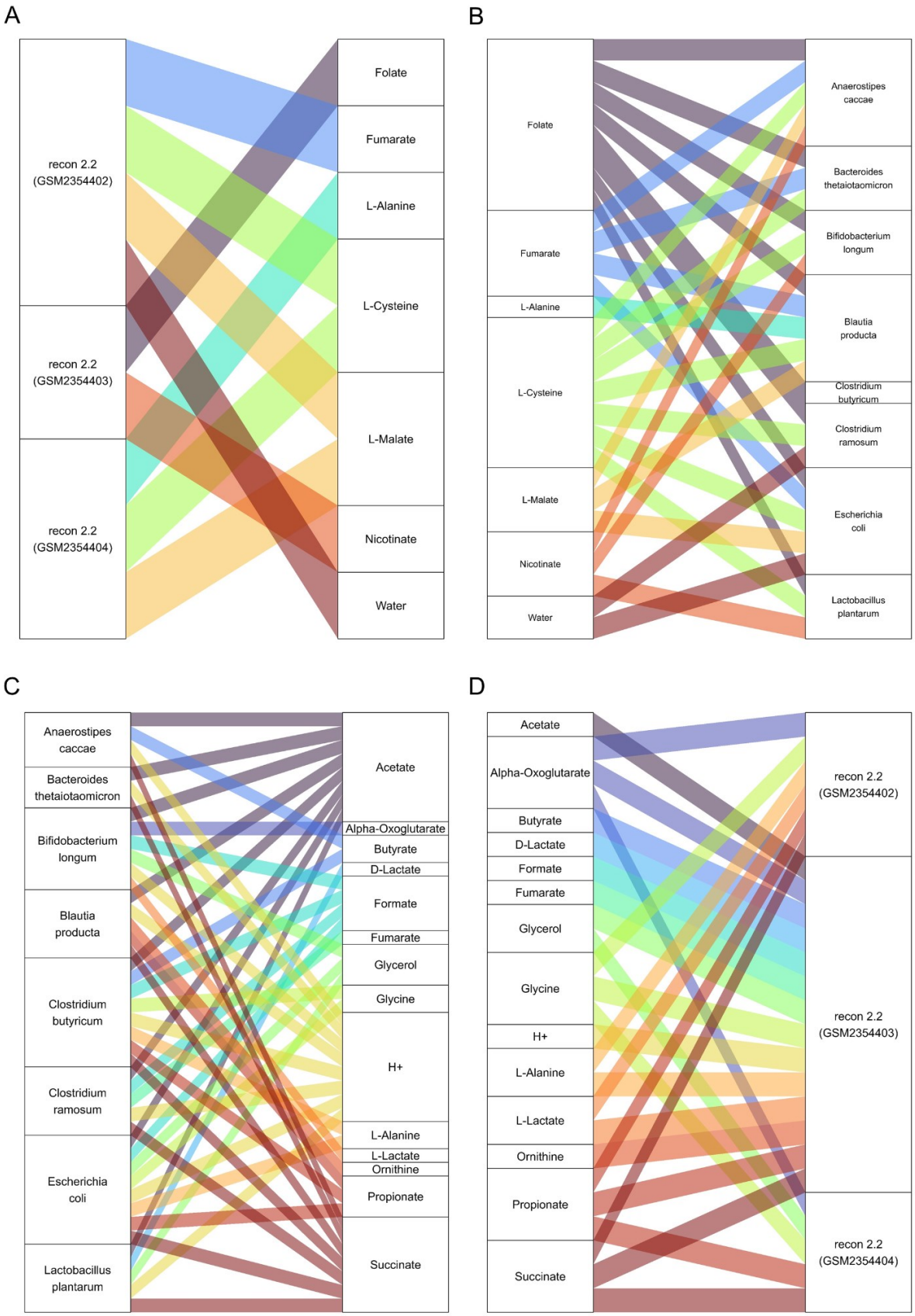

Figure 4: Schematic representation of compounds produced by the context-specific host models (A) and consumed by the SIHUMIx bacteria (B) along with the bacterially produced

ones (C) that are consumed by the host models (D). Metabolites with the highest interaction frequency (>= 50%) across all time points and simulations were selected to be plotted for simplicity. For the full dataset, see Supplementary Table S3.

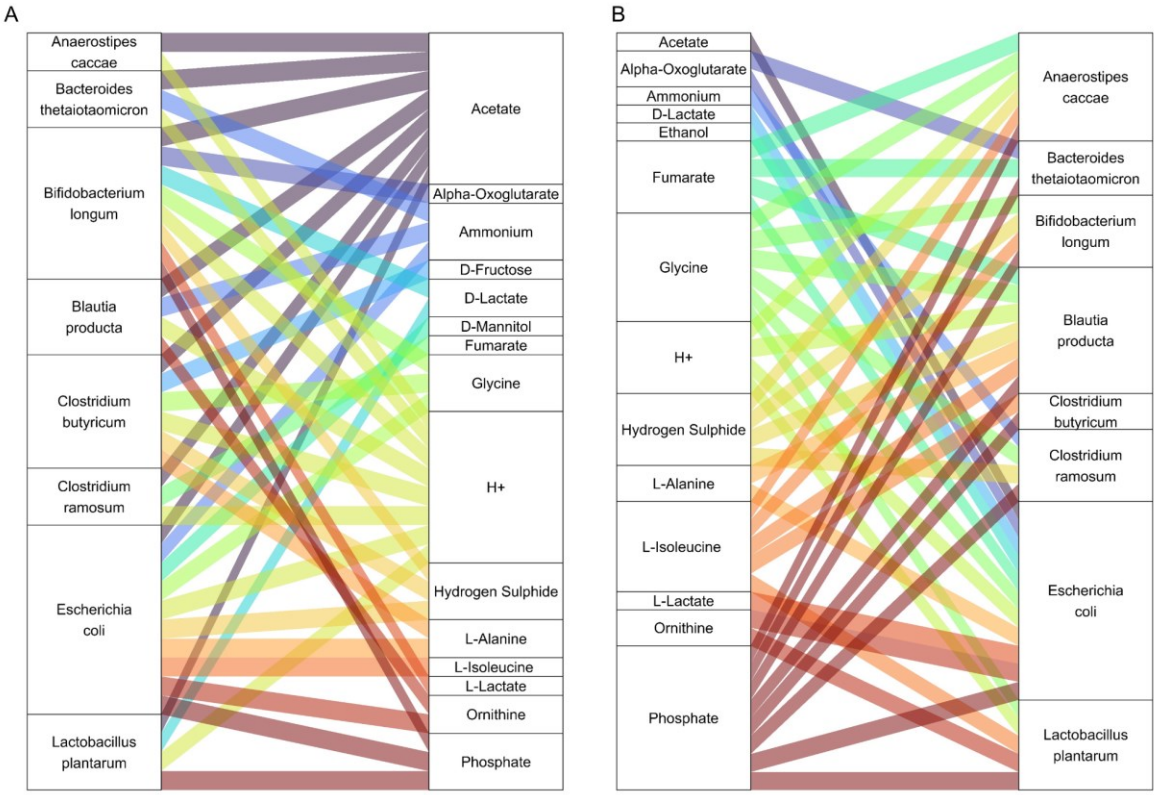

Figure 5: Schematic representation of compounds produced by the SIHUMIx bacterial models (A) and consumed by other SIHUMIx bacterial models (B). Metabolites with the highest interaction frequency (>= 50%) across all time points and simulations were selected to be plotted for simplicity. For the full dataset, see Supplementary Table S3.

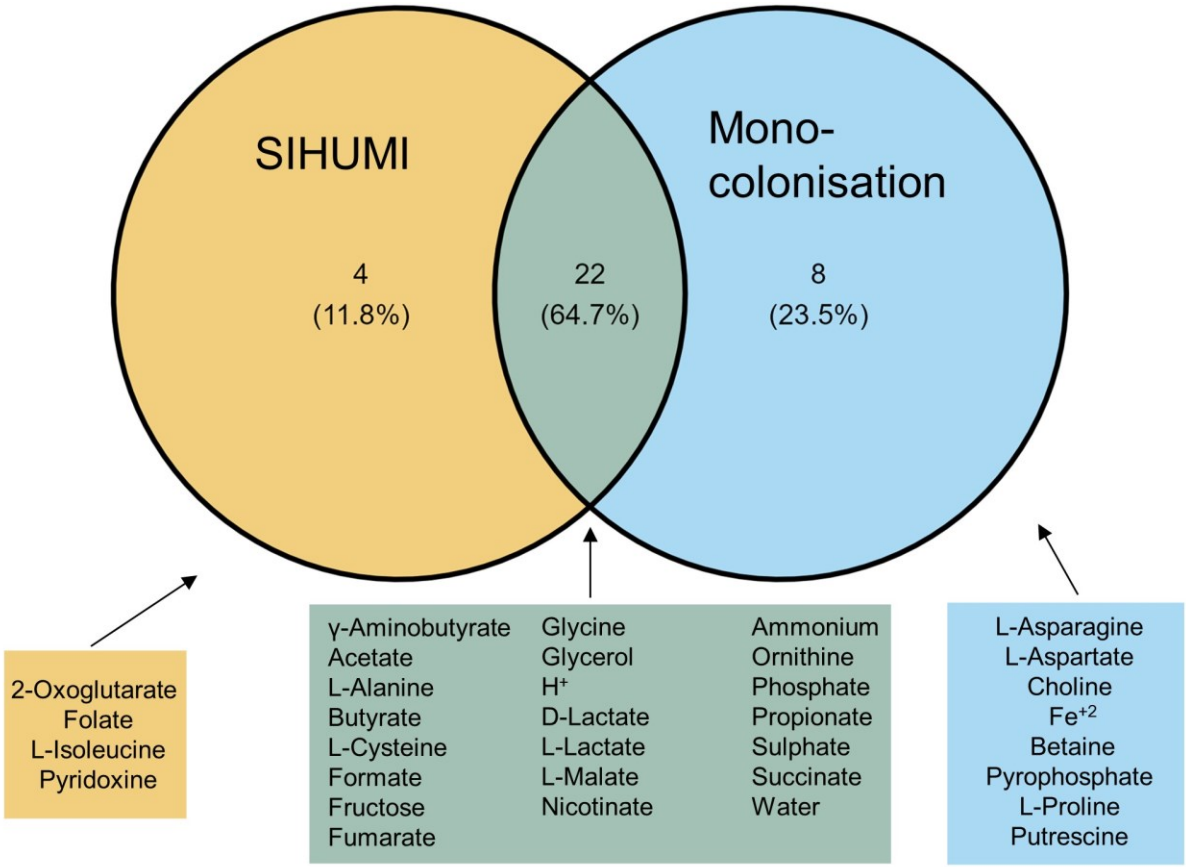

Figure 6: Schematic representation of compounds exchanged by the bacterial models and host models in the mono-colonisation and SIHUMIx experiments. Only interactions with bacteria from the shared genera were taken into account (*Bacteroides, Bifidobacterium, Clostridium, Lactobacillus*). All simulation time points were included in the analysis.

Table 2: Comparison of Virtual Colon with other published approaches

Name	Approach	Microbes	Scope	Host	Space	Time	Mucus	Gut motility	Availability	Ref
Gut-Microbiota	PDE model with fluid dynamics (Stokes)	Movement + predefined functions	Colon	Nutrient uptake	✓	✓	✓	✓	Matlab https://forgemia.inra.fr/simon.labarthe/gut-microbiota	[65]
MicroGutPop	ODE model (Monod equation)	predefined functional groups	Colon	-	-	✓	✓	✓	R https://github.com/HelenKettle/microPopGutCode	[66]
GutLogo	ABM		Ileum	-	✓	✓	✓	✓	https://github.com/GutLogo/GutLogo	[67]
Synthetic Gut Microbiome	ODE model (gLV)	25 microbes	Butyrate production	-	-	✓	-	-	Julia https://github.com/RyanLincolnClark/DesignSyntheticGutMicrobiomeAssemblyFunction	[68]
Virtual Colon	ABM + PDE	Movement + metabolic model	Colon	Metabolic model	✓	✓	✓	✓	R http://www.github.com/maringos/VirtualColon	this study

PDE: Partial differential equation; ODE: Ordinary differential equations; gLV: generalised Lotka-Volterra; ABM: Agent-based modelling;
Ref: Reference

5. Discussion

Host-bacterial metabolic interactions are considered important drivers of host health and fitness. Therefore, one of the objectives of this study was to develop a data-driven approach that allows us to systematically explore the compounds that are exchanged between the host and bacterial cells. Here we present the Virtual Colon that extends the agent-based modelling framework BacArena[16,31] to study host-microbiome interactions in the mammalian large intestine. Specifically, it enables host-microbial simulations, in which bacteria and host cells are spatially separated through multilayer mucus layers. Moreover, it includes spatial-dependent diffusion that constrains substrate availability for the models. Most importantly, it not only enables the joint simulation of host and microbial interactions but also visualises them. While other methods have contributed to the field either by using

differential equations and/or agent-based modelling (Table 2), the Virtual Colon, which is built on BacArena, combines them in one software framework.

In our simulations, we utilised host models that originated from the human model Recon 2.2[36]. For the simulations, the host models were adapted using transcriptomic data[38] from mono-colonisation experiments of germ-free mice with the respective species[32]. In the case of colonisation with non-specific pathogens, we used the SIHUMIx bacterial models that comprise a generic eight-species human intestinal bacterial community[34].

To continue with the host-bacterial interactions in the mono-colonisation experiments, the observed usage of cysteine by some bacteria of the genus *Fusobacterium* and *Clostridium* is in line with the literature, which proposes that cysteine is metabolised by bacteria, leading to hydrogen sulphide[69]. Hydrogen sulphide has been characterised as a compound with multiple effects, as in low levels, it supports colonic health, while in excess, it is associated with inflammatory and pathological states (e.g., inflammatory bowel disease and cancer)[69].

Additionally, the compound 4-aminobutanoate, also known as γ-aminobutyric acid (GABA), is predicted to be produced by *Lactobacillus rhamnosus* and *Bacteroides finegoldi* and be consumed by the host models, which is in accordance with the literature[70]. This compound may act on the central nervous system as well as the enteric nervous system of the host as part of the microbiota-gut-brain axis[70]. On the other hand, *Bacteroides finegoldi* has not been reported to be a GABA producer. However, a recent article proposed that the Bacteroides species can produce this molecule, although, in the simulations, no other *Bacteroides* species did so[71].

Recently, a study based on metabolomics focusing on the colonic absorption of compounds with low molecular weight in mice identified some of the computationally predicted compounds, which were subject to metabolic exchange in our simulations: (glycine) betaine, choline, alanine, glutamine, glycine, isoleucine, lactate, ornithine, and short-chain fatty acids (Fig. 2A, B)[72]. Interestingly, host-derived glycine betaine and choline can be further bacterially metabolised to trimethylamine-N-oxide and trimethylamine, for which a linkage to atherosclerotic cardiovascular disease has been demonstrated[73].

While mono-colonisation experiments offered a detailed overview of pairwise host-bacterial interactions, the bacterial species found in the mammalian colon are quite diverse. Therefore, we selected the representative SIHUMIx community to investigate how our results change in the context of a more complex community. Our simulations showed a wide exchange of compounds among the species as well as between bacteria and host cells. Not surprisingly, many byproducts were found also in mono-colonisations, implying that the repertoire of metabolic exchanges may be genera-dependent (Fig 6). The bacterial models create a complex web of compounds, where carbohydrate and amino acid metabolism as well as cofactors (e.g. vitamins) and byproducts are the most common end products. This observation becomes intriguing, if one considers that carbohydrates rather than amino acids are primarily used in bacterial energy metabolism, as amino acid metabolism is less cost-effective[74]. Moreover, this finding suggests that mono-colonisation experiments only partially capture interactions that can be observed in community colonisation, as the metabolic repertoire and signature may alter significantly.

It must be stated that the predicted exchange of compounds between the host and the bacterial models is based on the assumption that the host colonic cells can exchange compounds from the luminal side of the colon. For instance, amino acids are known to be

absorbed in the small intestine, while their absorption fate in the large intestine is unclear. While the colonic bacteria can metabolise the remaining amino acids, it is proposed that some of them can be used by colonocytes [75]. In parallel, it has been shown that colonocytes can excrete amino acids (e.g., alanine, aspartate, asparagine, isoleucine, and valine) in both apical and basolateral directions in vitro[76]. Therefore, the observed production or consumption of several compounds by the host is feasible and waits for further experimental validation. These experiments should investigate the transport of metabolites across the intestinal barrier. Such a pivotal set of experiments was performed by Li and colleagues, who identified gut species that deplete and metabolise amino acids throughout the intestine and therefore regulate host metabolism [77].

Furthermore, the Virtual Colon includes spatial parameters tailored to the large intestinal environment. For instance, the diffusion of compounds inside the mucus layer is limited and the bacteria in the inner mucus cannot move unless mucus is consumed by community members, such as *B. thetaiotaomicron*, a known mucus-degrading species [78](Fig 3). Additionally, our results proposed that there are spatial, localised interactions, therefore it could be suggested that the mucus layers can affect bacterial metabolism. (Fig 2B). In line with those observations, the growth rates across all bacteria in the outer mucus layer seem to be the ones in the lumen, while the rates in the inner mucus layer are the slowest (Fig 3B). Therefore, the simulation data suggests that our mucus both resembles the function of the mucus as a physical barrier and to some extent as a nutrient pool for the bacteria [9].

While the setting of the Virtual Colon recapitulates some of the observed host-microbial functions, there is also room for further expansions in the simulation setting. Future computational experiments may include more complex bacterial communities along with an improved representation of the abundance of bacteria with respect to the size of the simulated colon (e.g., the ratio of microbial abundance over the number of host models). Currently, the virtual gut represents the host model as the same size as bacterial models due to the technical limitations of BacArena. Another improvement could include metabolomic data from colonic tissue and lumen so that the chemical environment is as realistic as possible. Additionally, single-cell transcriptomics would allow the representation of the various cell types of the host tissue. To improve the realism of the simulations, the Virtual Colon also has the capacity to mimic the lumen faeces stream powered by peristalsis activities, to mimic the replenishment of mucus compounds through time or to initiate simulation assuming a non-empty colonic environment. Also it would be interesting to investigate whether the variability observed in our simulations recapitulates inter-individual variances in microbiome composition in mice.

In summary, our novel simulation framework, Virtual Colon, builds upon the popular BacArena platform to create a comprehensive tool for studying host-microbe interactions in the colon. By spatially separating bacteria and host cells and incorporating multilayer mucus representation, the Virtual Colon enables the realistic simulation of host-microbial interactions. This is achieved through a spatial-dependent diffusion mechanism that constrains substrate availability and accurately mimics the faecal stream. Furthermore, the Virtual Colon allows for the joint simulation of host and microbial interactions, which we demonstrated for human gut microbiome communities and personalised host models using transcriptomicomics data. Thus, Virtual Colon allows for the personalised modelling of host-microbiome-interactions given that host transcriptomic and compositional microbiome information is available. Notably, we employed the Virtual Colon to identify species-specific mucus layer degradation and amino acid exchange between microbes and host, providing

valuable insights into the intricate dynamics of the gut ecosystem. Our freely available software on GitHub invites future researchers to adapt and expand its capabilities to advance host-microbe interaction studies.

6. Authors' Contribution

Conceptualisation: GM, JZ
Methodology: GM, JZ, JT, CK
Software: GM, JZ
Formal analysis: GM
Investigation: GM, JZ, JT
Resources: CK
Data Curation: GM
Writing - Original Draft: GM, JZ
Writing - Review & Editing: All co-authors
Visualisation: GM
Supervision: CK, JZ
Project administration: GM
Funding acquisition: CK

7. Acknowledgements

CK acknowledges support from the German Research Foundation for the support through the collaborative research centre 1182 Origin and Function of Metaorganisms (sub-project A1), the research unit miTarget (FOR5042), and the excellence cluster "Precision medicine in chronic inflammation" (EXC2167) and additionally the German Ministry for Education and Research (E:Med iTREAT, support code 01ZX1902A). This research was supported in part through high-performance computing resources available at the Kiel University Computing Centre. The authors thank Dr Ahmed Samer Kadib Alban for providing them with critical opinions on the manuscript. Artificial Intelligence was utilised in improving the readability and clarity of the article, which was reviewed and approved by the co-authors.

8. Conflict of Interest

The authors declare that there are no conflicts of interest.

9. Supplementary Information

The software is freely available on GitHub (www.github.com/maringos/VirtualColon, commit: 0e56bda). The supporting files, as well as the mono-colonisation simulation files (folder 'Supplementary Data S3') and the SIHUMIx simulation files (folder 'Supplementary Data S4'), which are related to this manuscript, can be found on Figshare (www.doi.org/10.6084/m9.figshare.29282060).

10. References

1. Ruuskanen, M.O., Sommeria-Klein, G., Havulinna, A.S., Niiranen, T.J., and Lahti, L. (2021). Modelling spatial patterns in host-associated microbial communities. Env. Microbiol *23*, 2374–2388. https://doi.org/10.1111/1462-2920.15462.

2. Hou, K., Wu, Z.-X., Chen, X.-Y., Wang, J.-Q., Zhang, D., Xiao, C., Zhu, D., Koya, J.B., Wei, L., Li, J., et al. (2022). Microbiota in health and diseases. Signal Transduct. Target. Ther. *7*, 135. https://doi.org/10.1038/s41392-022-00974-4.

3. Morrison, D.J., and Preston, T. (2016). Formation of short chain fatty acids by the gut microbiota and their impact on human metabolism. Gut Microbes *7*, 189–200. https://doi.org/10.1080/19490976.2015.1134082.

4. Shimizu, H., Masujima, Y., Ushiroda, C., Mizushima, R., Taira, S., Ohue-Kitano, R., and Kimura, I. (2019). Dietary short-chain fatty acid intake improves the hepatic metabolic condition via FFAR3. Sci Rep *9*, 16574. https://doi.org/10.1038/s41598-019-53242-x.

5. Van Treuren, W., and Dodd, D. (2020). Microbial Contribution to the Human Metabolome: Implications for Health and Disease. Annu. Rev. Pathol. Mech. Dis. *15*, 345–369. https://doi.org/10.1146/annurev-pathol-020117-043559.

6. Donohoe, D.R., Garge, N., Zhang, X., Sun, W., O'Connell, T.M., Bunger, M.K., and Bultman, S.J. (2011). The Microbiome and Butyrate Regulate Energy Metabolism and Autophagy in the Mammalian Colon. Cell Metab. *13*, 517–526. https://doi.org/10.1016/j.cmet.2011.02.018.

7. Yao, Y., Cai, X., Fei, W., Ye, Y., Zhao, M., and Zheng, C. (2022). The role of short-chain fatty acids in immunity, inflammation and metabolism. Crit. Rev. Food Sci. Nutr. *62*, 1–12. https://doi.org/10.1080/10408398.2020.1854675.

8. Fogelson, K.A., Dorrestein, P.C., Zarrinpar, A., and Knight, R. (2023). The Gut Microbial Bile Acid Modulation and Its Relevance to Digestive Health and Diseases. Gastroenterology *164*, 1069–1085. https://doi.org/10.1053/j.gastro.2023.02.022.

9. Schroeder, B.O. (2019). Fight them or feed them: how the intestinal mucus layer manages the gut microbiota. Gastroenterol Rep *7*, 3–12. https://doi.org/10.1093/gastro/goy052.

10. Konjar, Š., Pavšič, M., and Veldhoen, M. (2021). Regulation of Oxygen Homeostasis at the Intestinal Epithelial Barrier Site. Int J Mol Sci *22*. https://doi.org/10.3390/ijms22179170.

11. Litvak, Y., Byndloss, M.X., and Bäumler, A.J. (2018). Colonocyte metabolism shapes the gut microbiota. Science *362*. https://doi.org/10.1126/science.aat9076.

12. O'Keefe, S.J.D. (2016). Diet, microorganisms and their metabolites, and colon cancer. Nat Rev Gastroenterol Hepatol *13*, 691–706. https://doi.org/10.1038/nrgastro.2016.165.

13. Cremer, J., Arnoldini, M., and Hwa, T. (2017). Effect of water flow and chemical environment on microbiota growth and composition in the human colon. Proc. Natl.

Acad. Sci. *114*, 6438–6443. https://doi.org/10.1073/pnas.1619598114.

14. Mendoza, S.N., Olivier, B.G., Molenaar, D., and Teusink, B. (2019). A systematic assessment of current genome-scale metabolic reconstruction tools. Genome Biol *20*, 158. https://doi.org/10.1186/s13059-019-1769-1.

15. Zimmermann, J., Kaleta, C., and Waschina, S. (2021). gapseq: informed prediction of bacterial metabolic pathways and reconstruction of accurate metabolic models. Genome Biol *22*, 81. https://doi.org/10.1186/s13059-021-02295-1.

16. Jansma, J., and El Aidy, S. (2021). Understanding the host-microbe interactions using metabolic modeling. Microbiome *9*, 16. https://doi.org/10.1186/s40168-020-00955-1.

17. Orth, J.D., Thiele, I., and Palsson, B.Ø. (2010). What is flux balance analysis? Nat Biotechnol *28*, 245–248. https://doi.org/10.1038/nbt.1614.

18. Orth, J.D., Fleming, R.M.T., and Palsson, B.Ø. (2010). Reconstruction and Use of Microbial Metabolic Networks: the Core *Escherichia coli* Metabolic Model as an Educational Guide. EcoSal Plus *4*, 10.1128/ecosalplus.10.2.1. https://doi.org/10.1128/ecosalplus.10.2.1.

19. Heinken, A., Hertel, J., Acharya, G., Ravcheev, D.A., Nyga, M., Okpala, O.E., Hogan, M., Magnúsdóttir, S., Martinelli, F., Nap, B., et al. (2023). Genome-scale metabolic reconstruction of 7,302 human microorganisms for personalized medicine. Nat. Biotechnol. *41*, 1320–1331. https://doi.org/10.1038/s41587-022-01628-0.

20. Machado, D., Andrejev, S., Tramontano, M., and Patil, K.R. (2018). Fast automated reconstruction of genome-scale metabolic models for microbial species and communities. Nucleic Acids Res. *46*, 7542–7553. https://doi.org/10.1093/nar/gky537.

21. Noronha, A., Modamio, J., Jarosz, Y., Guerard, E., Sompairac, N., Preciat, G., Daníelsdóttir, A.D., Krecke, M., Merten, D., Haraldsdóttir, H.S., et al. (2019). The Virtual Metabolic Human database: integrating human and gut microbiome metabolism with nutrition and disease. Nucleic Acids Res. *47*, D614–D624. https://doi.org/10.1093/nar/gky992.

22. Ganter, M., Bernard, T., Moretti, S., Stelling, J., and Pagni, M. (2013). MetaNetX.org: a website and repository for accessing, analysing and manipulating metabolic networks. Bioinformatics *29*, 815–816. https://doi.org/10.1093/bioinformatics/btt036.

23. Bernard, T., Bridge, A., Morgat, A., Moretti, S., Xenarios, I., and Pagni, M. (2014). Reconciliation of metabolites and biochemical reactions for metabolic networks. Brief. Bioinform. *15*, 123–135. https://doi.org/10.1093/bib/bbs058.

24. Moretti, S., Martin, O., Van Du Tran, T., Bridge, A., Morgat, A., and Pagni, M. (2016). MetaNetX/MNXref – reconciliation of metabolites and biochemical reactions to bring together genome-scale metabolic networks. Nucleic Acids Res. *44*, D523–D526. https://doi.org/10.1093/nar/gkv1117.

25. Moretti, S., Tran, V.D.T., Mehl, F., Ibberson, M., and Pagni, M. (2021). MetaNetX/MNXref: unified namespace for metabolites and biochemical reactions in the context of metabolic models. Nucleic Acids Res. *49*, D570–D574. https://doi.org/10.1093/nar/gkaa992.

26. Kanehisa, M. (2000). KEGG: Kyoto Encyclopedia of Genes and Genomes. Nucleic Acids

Res. *28*, 27–30. https://doi.org/10.1093/nar/28.1.27.

27. Kanehisa, M. (2019). Toward understanding the origin and evolution of cellular organisms. Protein Sci. *28*, 1947–1951. https://doi.org/10.1002/pro.3715.

28. Kanehisa, M., Furumichi, M., Sato, Y., Kawashima, M., and Ishiguro-Watanabe, M. (2023). KEGG for taxonomy-based analysis of pathways and genomes. Nucleic Acids Res. *51*, D587–D592. https://doi.org/10.1093/nar/gkac963.

29. Scott, W.T., Benito-Vaquerizo, S., Zimmermann, J., Bajić, D., Heinken, A., Suarez-Diez, M., and Schaap, P.J. (2023). A structured evaluation of genome-scale constraint-based modeling tools for microbial consortia. PLOS Comput. Biol. *19*, e1011363. https://doi.org/10.1371/journal.pcbi.1011363.

30. Versluis, D.M., Schoemaker, R., Looijesteijn, E., Muysken, D., Jeurink, P.V., Paques, M., Geurts, J.M.W., and Merks, R.M.H. (2022). A Multiscale Spatiotemporal Model Including a Switch from Aerobic to Anaerobic Metabolism Reproduces Succession in the Early Infant Gut Microbiota. mSystems *7*, e00446-22. https://doi.org/10.1128/msystems.00446-22.

31. Bauer, E., Zimmermann, J., Baldini, F., Thiele, I., and Kaleta, C. (2017). BacArena: Individual-based metabolic modeling of heterogeneous microbes in complex communities. PLoS Comput Biol *13*, e1005544. https://doi.org/10.1371/journal.pcbi.1005544.

32. Geva-Zatorsky, N., Sefik, E., Kua, L., Pasman, L., Tan, T.G., Ortiz-Lopez, A., Yanortsang, T.B., Yang, L., Jupp, R., Mathis, D., et al. (2017). Mining the Human Gut Microbiota for Immunomodulatory Organisms. Cell *168*, 928-943.e11. https://doi.org/10.1016/j.cell.2017.01.022.

33. Lewis, N.E., Hixson, K.K., Conrad, T.M., Lerman, J.A., Charusanti, P., Polpitiya, A.D., Adkins, J.N., Schramm, G., Purvine, S.O., Lopez-Ferrer, D., et al. (2010). Omic data from evolved *E. coli* are consistent with computed optimal growth from genome-scale models. Mol. Syst. Biol. *6*, 390. https://doi.org/10.1038/msb.2010.47.

34. Becker, N., Kunath, J., Loh, G., and Blaut, M. (2011). Human intestinal microbiota: Characterization of a simplified and stable gnotobiotic rat model. Gut Microbes *2*, 25–33. https://doi.org/10.4161/gmic.2.1.14651.

35. Fritzenwanker, M., Hain, T., Kesper, D.A., Harb, H., Renz, H., and Domann, E. (2016). Draft Genome Sequence and Complete Plasmid Sequence of *Acinetobacter lwoffii* F78, an Isolate with Strong Allergy-Protective Properties. Genome Announc. *4*, e00685-16. https://doi.org/10.1128/genomeA.00685-16.

36. Swainston, N., Smallbone, K., Hefzi, H., Dobson, P.D., Brewer, J., Hanscho, M., Zielinski, D.C., Ang, K.S., Gardiner, N.J., Gutierrez, J.M., et al. (2016). Recon 2.2: from reconstruction to model of human metabolism. Metabolomics *12*, 109. https://doi.org/10.1007/s11306-016-1051-4.

37. Sahoo, S., and Thiele, I. (2013). Predicting the impact of diet and enzymopathies on human small intestinal epithelial cells. Hum. Mol. Genet. *22*, 2705–2722. https://doi.org/10.1093/hmg/ddt119.

38. Gene Expression Omnibus Accession Viewer GSE88919. https://www.ncbi.nlm.nih.gov/geo/query/acc.cgi? acc=GSE88919

https://www.ncbi.nlm.nih.gov/geo/query/acc.cgi? acc=GSE88919.

39. Zur, H., Ruppin, E., and Shlomi, T. (2010). iMAT: an integrative metabolic analysis tool. Bioinformatics *26*, 3140–3142. https://doi.org/10.1093/bioinformatics/btq602.

40. Khodaee, S., Asgari, Y., Totonchi, M., and Karimi-Jafari, M.H. (2020). iMM1865: A New Reconstruction of Mouse Genome-Scale Metabolic Model. Sci. Rep. *10*, 6177. https://doi.org/10.1038/s41598-020-63235-w.

41. Gustafsson, J.K., Ermund, A., Johansson, M.E.V., Schütte, A., Hansson, G.C., and Sjövall, H. (2012). An ex vivo method for studying mucus formation, properties, and thickness in human colonic biopsies and mouse small and large intestinal explants. Am. J. Physiol.-Gastrointest. Liver Physiol. *302*, G430–G438. https://doi.org/10.1152/ajpgi.00405.2011.

42. Johansson, M.E.V., Phillipson, M., Petersson, J., Velcich, A., Holm, L., and Hansson, G.C. (2008). The inner of the two Muc2 mucin-dependent mucus layers in colon is devoid of bacteria. Proc. Natl. Acad. Sci. *105*, 15064–15069. https://doi.org/10.1073/pnas.0803124105.

43. Casteleyn, C., Rekecki, A., Van Der Aa, A., Simoens, P., and Van Den Broeck, W. (2010). Surface area assessment of the murine intestinal tract as a prerequisite for oral dose translation from mouse to man. Lab. Anim. *44*, 176–183. https://doi.org/10.1258/la.2009.009112.

44. De Rodriguez, M.S.B., Sunter, J.P., Watson, A.J., Wright, N.A., and Appleton, D.R. (1978). Cell population kinetics in the mucosal crypts of the descending colon of the mouse. Virchows Arch. B Cell Pathol. *29*, 351–361. https://doi.org/10.1007/BF02899366.

45. Milo, R., Jorgensen, P., Moran, U., Weber, G., and Springer, M. (2010). BioNumbers—the database of key numbers in molecular and cell biology. Nucleic Acids Res. *38*, D750–D753. https://doi.org/10.1093/nar/gkp889.

46. Park, J., Kotani, T., Konno, T., Setiawan, J., Kitamura, Y., Imada, S., Usui, Y., Hatano, N., Shinohara, M., Saito, Y., et al. (2016). Promotion of Intestinal Epithelial Cell Turnover by Commensal Bacteria: Role of Short-Chain Fatty Acids. PLOS ONE *11*, e0156334. https://doi.org/10.1371/journal.pone.0156334.

47. Winne, D., and Verheyen, W. (1990). Diffusion coefficient in native mucus gel of rat small intestine. J. Pharm. Pharmacol. *42*, 517–519. https://doi.org/10.1111/j.2042-7158.1990.tb06611.x.

48. Pappenheimer, J.R., and Reiss, K.Z. (1987). Contribution of solvent drag through intercellular junctions to absorption of nutrients by the small intestine of the rat. J. Membr. Biol. *100*, 123–136. https://doi.org/10.1007/BF02209145.

49. Wishart, D.S., Tzur, D., Knox, C., Eisner, R., Guo, A.C., Young, N., Cheng, D., Jewell, K., Arndt, D., Sawhney, S., et al. (2007). HMDB: the Human Metabolome Database. Nucleic Acids Res. *35*, D521–D526. https://doi.org/10.1093/nar/gkl923.

50. Wishart, D.S., Knox, C., Guo, A.C., Eisner, R., Young, N., Gautam, B., Hau, D.D., Psychogios, N., Dong, E., Bouatra, S., et al. (2009). HMDB: a knowledgebase for the human metabolome. Nucleic Acids Res. *37*, D603–D610. https://doi.org/10.1093/nar/gkn810.

51. Wishart, D.S., Jewison, T., Guo, A.C., Wilson, M., Knox, C., Liu, Y., Djoumbou, Y., Mandal, R., Aziat, F., Dong, E., et al. (2012). HMDB 3.0—The Human Metabolome Database in 2013. Nucleic Acids Res. *41*, D801–D807. https://doi.org/10.1093/nar/gks1065.

52. Wishart, D.S., Feunang, Y.D., Marcu, A., Guo, A.C., Liang, K., Vázquez-Fresno, R., Sajed, T., Johnson, D., Li, C., Karu, N., et al. (2018). HMDB 4.0: the human metabolome database for 2018. Nucleic Acids Res. *46*, D608–D617. https://doi.org/10.1093/nar/gkx1089.

53. R Core Team R: A Language and Environment for Statistical Computing. (R Foundation for Statistical Computing).

54. Gelius-Dietrich, G., Desouki, A.A., Fritzemeier, C.J., and Lercher, M.J. (2013). sybil – Efficient constraint-based modelling in R. BMC Syst. Biol. *7*, 125. https://doi.org/10.1186/1752-0509-7-125.

55. IBM IBM ILOG CPLEX Optimization Studio.

56. Gelius-Dietrich, G. cplexAPI: R Interface to C API of IBM ILOG CPLEX.

57. Wickham, H., Averick, M., Bryan, J., Chang, W., McGowan, L., François, R., Grolemund, G., Hayes, A., Henry, L., Hester, J., et al. (2019). Welcome to the Tidyverse. J. Open Source Softw. *4*, 1686. https://doi.org/10.21105/joss.01686.

58. Wickham, H., François, R., Henry, L., Müller, K., and Vaughan, D. dplyr: A Grammar of Data Manipulation.

59. Wickham, H. (2016). ggplot2: Elegant Graphics for Data Analysis (Springer-Verlag New York).

60. Linlin, Y. ggvenn: Draw Venn Diagram by “ggplot2.”

61. Arnold, J.B. ggthemes: Extra Themes, Scales and Geoms for “ggplot2.”

62. Wickham, H., and Seidel, D. scales: Scale Functions for Visualization.

63. Brunson, J. (2020). ggalluvial: Layered Grammar for Alluvial Plots. J. Open Source Softw. *5*, 2017. https://doi.org/10.21105/joss.02017.

64. Wickham, H., Hester, J., Chang, W., and Bryan, J. devtools: Tools to Make Developing R Packages Easier.

65. Labarthe, S., Polizzi, B., Phan, T., Goudon, T., Ribot, M., and Laroche, B. (2019). A mathematical model to investigate the key drivers of the biogeography of the colon microbiota. J. Theor. Biol. *462*, 552–581. https://doi.org/10.1016/j.jtbi.2018.12.009.

66. Kettle, H., Louis, P., and Flint, H.J. (2022). Process-based modelling of microbial community dynamics in the human colon. J. R. Soc. Interface *19*, 20220489. https://doi.org/10.1098/rsif.2022.0489.

67. Lin, C., Culver, J., Weston, B., Underhill, E., Gorky, J., and Dhurjati, P. (2018). GutLogo: Agent-based modeling framework to investigate spatial and temporal dynamics in the gut microbiome. PLOS ONE *13*, e0207072. https://doi.org/10.1371/journal.pone.0207072.

68. Clark, R.L., Connors, B.M., Stevenson, D.M., Hromada, S.E., Hamilton, J.J., Amador-

Noguez, D., and Venturelli, O.S. (2021). Design of synthetic human gut microbiome assembly and butyrate production. Nat. Commun. *12*, 3254. https://doi.org/10.1038/s41467-021-22938-y.

69. Blachier, F., Beaumont, M., and Kim, E. (2019). Cysteine-derived hydrogen sulfide and gut health: a matter of endogenous or bacterial origin. Curr. Opin. Clin. Nutr. Metab. Care *22*, 68–75. https://doi.org/10.1097/MCO.0000000000000526.

70. Yong, S.J., Tong, T., Chew, J., and Lim, W.L. (2020). Antidepressive Mechanisms of Probiotics and Their Therapeutic Potential. Front. Neurosci. *13*, 1361. https://doi.org/10.3389/fnins.2019.01361.

71. Otaru, N., Ye, K., Mujezinovic, D., Berchtold, L., Constancias, F., Cornejo, F.A., Krzystek, A., De Wouters, T., Braegger, C., Lacroix, C., et al. (2021). GABA Production by Human Intestinal Bacteroides spp.: Prevalence, Regulation, and Role in Acid Stress Tolerance. Front. Microbiol. *12*, 656895. https://doi.org/10.3389/fmicb.2021.656895.

72. Matsumoto, M., Ooga, T., Kibe, R., Aiba, Y., Koga, Y., and Benno, Y. (2017). Colonic Absorption of Low-Molecular-Weight Metabolites Influenced by the Intestinal Microbiome: A Pilot Study. PLOS ONE *12*, e0169207. https://doi.org/10.1371/journal.pone.0169207.

73. Canyelles, M., Borràs, C., Rotllan, N., Tondo, M., Escolà-Gil, J.C., and Blanco-Vaca, F. (2023). Gut Microbiota-Derived TMAO: A Causal Factor Promoting Atherosclerotic Cardiovascular Disease? Int. J. Mol. Sci. *24*, 1940. https://doi.org/10.3390/ijms24031940.

74. Oliphant, K., and Allen-Vercoe, E. (2019). Macronutrient metabolism by the human gut microbiome: major fermentation by-products and their impact on host health. Microbiome *7*, 91. https://doi.org/10.1186/s40168-019-0704-8.

75. Ma, N., and Ma, X. (2019). Dietary Amino Acids and the Gut-Microbiome-Immune Axis: Physiological Metabolism and Therapeutic Prospects. Compr. Rev. Food Sci. Food Saf. *18*, 221–242. https://doi.org/10.1111/1541-4337.12401.

76. Chen, Y., Dinges, M.M., Green, A., Cramer, S.E., Larive, C.K., and Lytle, C. (2020). Absorptive transport of amino acids by the rat colon. Am. J. Physiol.-Gastrointest. Liver Physiol. *318*, G189–G202. https://doi.org/10.1152/ajpgi.00277.2019.

77. Li, T.-T., Chen, X., Huo, D., Arifuzzaman, M., Qiao, S., Jin, W.-B., Shi, H., Li, X.V., Iliev, I.D., Artis, D., et al. (2024). Microbiota metabolism of intestinal amino acids impacts host nutrient homeostasis and physiology. Cell Host Microbe *32*, 661-675.e10. https://doi.org/10.1016/j.chom.2024.04.004.

78. Kostopoulos, I., Aalvink, S., Kovatcheva-Datchary, P., Nijsse, B., Bäckhed, F., Knol, J., De Vos, W.M., and Belzer, C. (2021). A Continuous Battle for Host-Derived Glycans Between a Mucus Specialist and a Glycan Generalist in vitro and in vivo. Front. Microbiol. *12*, 632454. https://doi.org/10.3389/fmicb.2021.632454.